



Research paper

Spray freeze drying for dry powder inhalation of nanoparticles

Mohamed Ehab Ali ^{a,b}, Alf Lamprecht ^{a,c,*}^a Laboratory of Pharmaceutical Technology and Biopharmaceutics, Institute of Pharmacy, University of Bonn, Bonn, Germany^b Department of Industrial Pharmacy, Faculty of Pharmacy, Assiut University, Assiut, Egypt^c Laboratory of Pharmaceutical Engineering, University of Franche-Comté, Besançon, France

ARTICLE INFO

Article history:

Received 3 December 2013

Accepted in revised form 14 March 2014

Available online 21 March 2014

Keywords:

Spray freeze drying

Spray drying

Pulmonary

Nanoparticles

Dry powder

Inhalation

Nanocomposite microcarriers

ABSTRACT

Formulating nanoparticles for delivery to the deep lung is complex and many techniques fail in terms of nanoparticle stability. Spray freeze drying (SFD) is suggested here for the production of inhalable nanocomposite microcarriers (NCM). Different nanostructures were prepared and characterized including polymeric and lipid nanoparticles. Nanoparticle suspensions were co-sprayed with a suitable cryoprotectant into a cooled, stainless steel spray tower, followed by freeze drying to form a dry powder while equivalent compositions were spray dried (SD) as controls. SFD-NCM possess larger specific surface areas (67–77 m²/g) and lower densities (0.02 g/cm³) than their corresponding SD-NCM. With the exception of NCM of lipid based nanocarriers, SFD produced NCM with a mass median aerodynamic diameter (MMAD) of 3.0 ± 0.5 μm and fine particle fraction (FPF ≤ 5.2 μm) of 45 ± 1.6% with aerodynamic performances similar to SD-NCM. However, SFD was superior to SD in terms of maintaining the particle size of all the investigated polymeric and lipid nanocarriers following reconstitution (S_f/S_r ratio for SFD ≈ 1 versus >1.5 for SD). The SFD into cooled air proved to be an efficient technique to prepare NCM for pulmonary delivery while maintaining the stability of the nanoparticles.

© 2014 Elsevier B.V. All rights reserved.

1. Introduction

Over the last decades, colloidal drug delivery systems and especially nanoparticles have received increasing attention. Nanosystems with different compositions and biological properties have been extensively investigated for drug, protein and gene delivery applications. Pulmonary delivery has become a popular method to deliver therapeutic or diagnostic compounds. This is due to the large alveolar surface area, the low thickness of the epithelial barrier and the extensive vascularization in the alveolar region

Abbreviations: SFD, spray freeze drying; SD, spray drying; NCM, nanocomposite microcarriers; NP, nanoparticles; PLGA, poly (DL-lactide-co-glycolide); EDRL, poly(meth)acrylate (Eudragit® RL PO); EC, ethyl cellulose; PVAL, polyvinyl alcohol; MCT, medium chain triglyceride; PVP, polyvinylpyrrolidone (kollidon 12 PF); LNC, lipid nanocapsules; SLN, solid lipid nanoparticles; PDI, polydispersity index; SEM, scanning electron microscope; d_{50} , volume median particle size; ρ_{bulk} , bulk density; ρ_{tapped} , tapped density; CI, Carr's compressibility index; NGI, next generation impactor; DPI, dry powder inhaler; MOC, micro-orifice contactor; RD, recovered dose; EF, emitted fraction; FPF, fine particle fraction; MMAD, mass median aerodynamic diameter; GSD, geometric standard deviation; S_f , particle size after reconstitution; S_r , particle size before reconstitution.

* Corresponding author. Laboratory of Pharmaceutical Technology and Biopharmaceutics, Institute of Pharmacy, University of Bonn, Bonn, Germany. Tel.: +49 228 735243.

E-mail address: alf.lamprecht@uni-bonn.de (A. Lamprecht).

[1,2]. The use of nanoparticles as therapeutic carriers for pulmonary delivery has gained significant interest because of their ability to enter the intracellular compartments and their bioavailability enhancement potential attributed to the unique ability of nanoparticles to evade the alveolar macrophages and mucociliary clearance mechanisms, resulting in prolonged drug residence time [3].

Nanoparticle delivery to the lungs suffers from two major drawbacks: firstly, nanoparticles, with the exception of particles <50 nm in size, are exhaled from the lungs [3]. Secondly, they show formulation instability due to their high surface energy, leading to aggregation and/or particle–particle interactions [4]. To overcome these problems, nanoparticles are often applied to the lungs in the form of suspensions. However, in this case, the size of the generated droplets will vary with the nebulizer technique and the applied stress during nebulization can affect the formulation stability [5]. The frequent instability problems of nanosuspensions, such as aggregation and/or drug leakage, can be overcome by applying nanoparticles as dry powder. Therefore, the production of nanocomposite microcarriers (NCM) has been suggested as a possible formulation strategy [6–8]. The formulation into a microsized carrier improves the stability and aerodynamic properties of the entrapped nanoparticles [9,10]. In this case, the size of the microcarrier determines the deposition in the lungs and is independent on the application device.

Spray drying (SD) is the commonly used technique to produce NCM within the aerodynamic diameter range suitable for pulmonary deposition [7–14]. One prominent concept was introduced by Tsapis et al. [15] who prepared an extremely thin-walled macro-scale structures by spray drying solutions of non-polymeric and polymeric nanoparticles. The solutes and nanoparticles accumulate at the evaporating front of the droplet and form a shell that dries to become the hollow microparticle. However, SD has some limitations regarding its use for heat sensitive materials and it requires precise adjustment of the inlet and outlet temperatures of the used hot gas. Alternatively, we propose here SFD for the production of inhalable NCM. In SFD, nanoparticle dispersions are atomized into a stainless steel spray tower encased by a cooling jacket of liquid nitrogen, so that the particles are frozen during the time of flight in the cold air, avoiding any contact with liquid nitrogen [16]. Additionally, a two-fluid nozzle was used to produce droplets of a size range suitable for pulmonary deposition. The two major prerequisites for these NCM are a significant lung deposition and a full reconstitution of nanoparticles when coming in contact with aqueous liquid, to maintain their beneficial therapeutic characteristics.

In this study, the feasibility of using SFD for preparing inhalable NCM of polymeric and lipid nanoparticles was investigated. Different polymeric and lipid nanostructures were prepared in order to test the effect of the nanocarrier type on the process of microcarrier formulation. Poly (DL-lactide-co-glycolide), Eudragit® RL and ethyl cellulose were investigated as polymer candidates for polymeric nanoparticles, while lipid nanocapsules and solid lipid nanoparticles were tested as lipid based nanocarriers. Afterward, the prepared polymeric and lipid nanostructures were co-spray freeze dried with maltodextrin and trehalose, respectively. Nevertheless, a comparative study was carried out with samples similarly prepared using SD technique. This comparison took into consideration: the production feasibility; the suitability of the prepared micro-carriers for pulmonary deposition; reconstitution ability of the NCM and nanoparticles size after reconstitution.

2. Experimental

2.1. Materials

Poly (DL-lactide-co-glycolide) (Resomer® RG 502 H; PLGA) was obtained from Boehringer Ingelheim, Germany. Poly(meth)acrylate: Eudragit® RL PO (EDRL) was a kind sample from Evonik Röhm GmbH, Darmstadt, Germany. Ethyl cellulose (Ethocel standard 4 premium, EC) was kind gift from Colorcon, UK. Miglyol® 812 (medium chain triglyceride, MCT) was from Fagron GmbH, Barsbüttel, Germany. Soybean lecithin and polysorbate 80 (Tween® 80) were purchased from Caelo, Germany. Witepsol® H15 was from Sasol GmbH, Witten, Germany. Polyvinyl alcohol (PVAL) 98–99% hydrolyzed and cholic acid sodium salt hydrate were purchased from Sigma–Aldrich Chemie GmbH, Steinheim, Germany. Maltodextrin (Roquette LAB 2509, dextrose equivalent of DE = 19) was a gift from Roquette Freres, Lestrem Cedex, France. Polyvinylpyrrolidone (kollidon 12 PF, *K*-value range = 10.2–13.8, PVP), Cremophor® A25 and Kolliphor® HS15 were kind samples from BASF, Ludwigshafen, Germany. Trehalose (Ph. Eur.) was purchased from VWR International, Amsterdam, Netherlands. All other chemicals were of analytical grade or equivalent purity.

2.2. Preparation of nanoparticles

Polymeric nanoparticles were prepared by the o/w emulsion solvent evaporation technique [17,18], using poly DL-lactide-co-glycolide (PLGA), ethyl cellulose (EC) or Eudragit RL (EDRL) as a polymer. 0.5 g. of each of the investigated polymers was dissolved

in 25 ml of either dichloromethane (for EDRL) or ethyl acetate (for PLGA and EC), forming the organic phase. This organic solution was then poured into 50 ml of the aqueous surfactant solution (0.1% sodium cholate for PLGA, 0.1% Tween 80 for EDRL, 1% PVAL for EC). The coarse emulsion formed was then further homogenized at 50 W for 5 min using ultrasonic cell disruptor (Banoelin sonopuls, Berlin, Germany). The solvent evaporation step was performed using a Büchi Rotavapor RE120 (Büchi, Flawil, Switzerland) for 20 min, reducing the pressure stepwise down to 30 mbar with a diaphragm pump.

Lipid nanocapsules (LNC) were prepared according to a solvent-free phase inversion method that allows the preparation of very small nanocapsules by thermal manipulation of oil/water system [19,20]. Briefly, 1 g. of the oil phase (triglyceride phase, MCT) was mixed with 1 g Kolliphor® HS15 and 3 g distilled water. Sodium chloride (100 mg) and soybean lecithin (100 mg) were also added. The mixture was heated under magnetic stirring up to 85 °C (until a distinct drop of conductivity occurs) to ensure that the phase inversion temperature was passed and a w/o emulsion was formed. Afterward, the emulsion was allowed to cool down to 55 °C on another magnetic stirrer. During cooling, another complete phase inversion to an o/w emulsion occurs. This cycle was repeated twice before adding 5 ml of distilled water at 4 °C. The LNC suspension was then stirred for 10 min before further analysis.

Solid lipid nanoparticles (SLN) were prepared by melting 10 g of the solid lipid Witepsol at 70 °C. The aqueous phase consisting of 90 ml water, containing 1 g sodium cholate and 2.5 g Cremophor® A25, was also heated to the same temperature and then added to the lipid melt followed by homogenization with ultraturax at 10,000 rpm for 10 min. The hot emulsion was then sonicated using ultrasonic cell disruptor (Banoelin sonopuls, Berlin, Germany) for 20 min at 70 °C and left overnight before further investigations [17,21].

2.3. Determination of the particle size

The prepared nanoparticles were analyzed for their particle size and size distribution in terms of the average volume diameters and polydispersity index (PDI) by photon correlation spectroscopy using particle size analyzer (Brookhaven Instruments Corporation, Holtsville, NY, USA) at fixed angle of 90° at 25 °C. The nanoparticle suspension was diluted with distilled water before particle size analysis. All samples were analyzed in triplicates at 25 °C and the error was calculated as standard deviation (SD).

2.4. Spray drying

Nanoparticle dispersions (1% w/v) were mixed with 5% w/v of either maltodextrin (for polymeric nanoparticles) or trehalose (for lipid nanocarriers) and 5% w/v PVP as stabilizers. The dispersions were then spray dried using a Büchi B-191 mini Spray Dryer (Büchi, Flawil, Switzerland) equipped with a two-fluid nozzle (0.7 mm). Spray drying was undertaken with the following settings: feed rate 3% (1 ml/min), inlet temperature 110 °C, air flow rate 750 NL/h and aspiration 85%. These settings resulted in an outlet temperature of 80 °C. Florescent microcarriers were prepared by incorporating 0.05% w/v sodium fluorescein in the aqueous suspension before spraying. The obtained powder was stored in vacuum desiccator over silica gel until used.

2.5. Spray freeze drying

SFD was carried out according to the method described by Eggerstedt et al. [16] with some modifications. Briefly, the process consisted of three steps: droplet formation, freezing, and freeze drying. For droplet formation, a two-fluid nozzle (0.7 mm) was

installed at the top of a spray tower. The freezing process was performed within a cooled, stainless steel spray tower encased by a cooling jacket of liquid nitrogen, where direct spraying into the liquid nitrogen was avoided by design. Nanoparticle dispersions (1% w/v) were co-sprayed with 5% w/v of either maltodextrin (for polymeric nanoparticles) or trehalose (for lipid nanocarriers) and 5% w/v PVP at a rate of 2 ml/min using an atomized air flow of 750 NL/h into a column of cold air at $-130\text{ }^{\circ}\text{C}$. The droplets are frozen in the cooled air and the frozen spherules are collected after sedimentation in a cooled container for further freeze drying. Florescent microcarriers were prepared by incorporating 0.05% w/v sodium fluorescein in the aqueous suspension before spraying. The frozen samples were lyophilized using a freeze dryer (STERIS Lyovac GT2, Hürth, Germany), where they are dried by a standard procedure for at least 36 h.

2.6. Physical characterization of the prepared NCM

2.6.1. Scanning electron microscope (SEM) analysis

SD- and SFD-NCM samples were mounted on double-sided adhesive tape, placed on aluminum stubs and sputter-coated (Polaron SC7640 Sputter Coater, Quorum Technologies Ltd., Newhaven, UK) for 4–6 min with gold and imaged with SEM (Hitachi S-2460N, Hitachi High Tech. Corp., Tokyo, Japan).

2.6.2. Particle size distribution

The geometric particle size distributions of the SD- and SFD-NCM were measured by laser diffraction spectrometry using a Sympatec Helos LF instrument. The Sympatec Rodos SD dispersing module (Sympatec GmbH, Clausthal-Zellerfeld, Germany) was used to disperse the samples into the measurement chamber at a pressure of 0.5 bar. Diffraction spectra were evaluated using the Fraunhofer theory option of Windox 3.4 software to calculate the volume median particle size (d_{50}). The span was then calculated as:

$$\text{Span} = d_{90} - d_{10}/d_{50} \quad (1)$$

Here d_{90} and d_{10} represent the diameters where 90% and 10% of the distribution has a smaller particle size, respectively. All measurements were performed in triplicate.

2.6.3. Bulk density and flowability

A known weight from each formulation was transferred to a 50 ml graduated cylinder and subjected to 1000 strokes using Erweka SVM 22 tap densitometer. By measuring both the initial apparent volume and the final tapped volume, the bulk (ρ_{bulk}) and tapped (ρ_{tapped}) densities were calculated.

The Carr's compressibility index (CI) is a measure of the flow properties of powders; and is calculated using the following equations:

$$\text{CI} = 100 \times [(\rho_{\text{tapped}} - \rho_{\text{bulk}})/\rho_{\text{tapped}}] \quad (2)$$

The smaller the Carr's index the better the flow properties. For example ≤ 10 indicates excellent, 11–15 good, 16–20 fair, 21–25 passable and > 25 poor flowability.

2.6.4. Specific surface area

The specific surface area was measured by Quantachrome Nova 3200 high speed gas sorption analyzer (Quantachrome, Boynton, FL, USA). The used adsorbate was nitrogen and the surface area was determined using the multipoint BET method from nitrogen adsorption isotherm at 77 K.

2.6.5. Aerodynamic properties

The aerodynamic properties of the prepared powders were determined using a Next Generation Impactor (NGI) (Copley

Scientific, Nottingham, UK). Particles dispersed in an air stream were conveyed through the instrument and impacted on the eight consecutive stages based on the well-characterized aerodynamic size cut-offs. The HandiHaler[®] DPI device (Boehringer Ingelheim, Germany) was attached to the NGI via a mouthpiece adaptor. Before each run, all stages were coated with 1% w/v silicon oil in n-hexane to minimize bouncing and re-entrainment of particles between stages. Five capsules (size 3), manually filled with 5–7 mg powder in each, were discharged from the DPI into the NGI. Using the critical flow controller (Copley Scientific, UK), the airflow rate is set at 45 L/min for 5.3 s to mimic 4 l of air drawn in human inhalation. The effective cut-off aerodynamic diameters for each stage at 45 L/min are 9.1, 5.2, 3.3, 1.9, 1.1, 0.6 and 0.4 μm for stages 1–7, respectively. After actuation, the contents of the capsules, DPI, mouthpiece adaptor, induction port, pre-separator, stages 1–7 and the micro-orifice contractor (MOC) were washed with deionised water into volumetric flasks and made up to volume. The fluorescence intensities of the solutions were measured by spectrofluorometry using 485 nm excitation filter and emission at 535 nm (Wallac 1420 Victor3 Multilabel counter, PerkinElmer). Each powder was tested in triplicate. Data were analyzed to calculate the recovered dose (RD; powder collected in the capsules, DPI, mouthpiece adaptor, induction port, pre-separator, stages 1–7 and MOC), the emitted fraction (EF; the fraction of powder that exited the inhaler with respect to the recovered dose) and the fine particle fraction (FPF; ratio of the recovered dose with cut-off aerodynamic diameter $\leq 5.2\text{ }\mu\text{m}$). A plot of cumulative percentage undersize versus effective cut-off diameter enabled determination of the mass median aerodynamic diameter (MMAD, diameter at 50% of the cumulative weight undersize), and the geometric standard deviation (GSD).

$$\text{GSD} = (d_{84\%}/d_{16\%})^{1/2} \quad (3)$$

where size d_n is the diameter at the percentile n of the cumulative distribution.

2.6.6. Reconstitution of nanoparticles from the prepared NCM

Briefly, 10 mg of the dried powder is reconstituted in 1 ml deionized water with gentle shaking to form a colloidal dispersion with subsequent measuring of the particle size after re-dispersion. Reconstitution ability was characterized from the change of the nanoparticle size before and after reconstitution. S_f is the average particle size after reconstitution, while S_i is the average particle size before drying. S_f/S_i ratio ≈ 1 denotes complete reconstitution, whereas S_f/S_i ratio > 1.5 denotes poor reconstitution [14,22].

3. Results

3.1. Nanoparticle preparation

Different nanostructures were prepared including polymeric and lipid nanoparticles. Results of particle size analysis are shown in Table 1. With the exception of SLN, particle design was optimized in order to obtain nanoparticles with average size $\leq 100\text{ nm}$, to be suitable as therapeutic carriers for pulmonary

Table 1
Size distribution of the prepared colloidal nanoparticles.

NP type	NP size distribution	
	Size (nm \pm SD)	PDI \pm SD
EC	111.4 \pm 10.2	0.11 \pm 0.01
EDRL	78.3 \pm 19.2	0.19 \pm 0.01
PLGA	81.7 \pm 11.5	0.10 \pm 0.01
SLN	441.8 \pm 7.5	0.18 \pm 0.02
LNC	36.2 \pm 2.6	0.07 \pm 0.02

delivery, being able to evade the alveolar macrophages and mucociliary clearance mechanisms. The prepared polymeric nanoparticles were in the size range from 78 ± 19.2 nm to 111 ± 10.2 nm and the average particle sizes of SLN and LNC were 441 ± 7.5 nm and 36 ± 2.6 nm, respectively.

3.2. NCM preparation

Based on preliminary studies, maltodextrin was selected as a suitable cryoprotectant for the polymeric nanoparticle samples while trehalose was selected for the lipid nanocarrier samples. For the polymeric nanoparticles, NCM preparation was possible by either SD or SFD. However, in case of lipid nanocarriers, NCM preparation was only possible using SFD. SD of LNC or SLN, owing to the high temperature employed, resulted in melting of the lipid core and cohesion of the melt droplets together as a waxy mass. The yields, as determined from the ratio of the NCM mass recovered after SD or SFD to the initial mass added to the feed, were $91.2 \pm 7.9\%$ w/w for SFD samples, and $68.6 \pm 8.4\%$ w/w for SD samples.

3.3. Morphology of NCM

SFD-NCM shows basically an interconnected porous surface (Fig. 1A). However, the addition of 5% PVP to the formulation tends to fill the void spaces between those interconnections giving hollow less porous particles (Fig. 1B). This improves the mechanical strength of the particles during handling, spraying and/or various measurements. SFD-NCM were spherical in shape (Fig. 2A–D), except the NCM of LNC which was irregular in shape (Fig. 2E). The difference between the SD- and SFD-NCM is clearly shown in the

SEM images. The SD-NCM were smaller with a slightly wrinkled smooth surface (Fig. 3A–C), while SFD particles were larger with a slightly rough surface (Fig. 2A–C).

3.4. Particle size analysis of NCM

Particle size distributions of SD- and SFD-NCM measured by laser diffraction analysis are shown in Table 2. The particle sizes observed under the SEM for the prepared NCM were corroborated by their corresponding laser diffraction data. Laser diffraction measurements revealed that the d_{50} of SD-NCM of polymeric nanoparticles ($d_{50} = 5\text{--}7$ μm) was smaller than that of the respective SFD-NCM ($d_{50} = 9\text{--}12$ μm). However, they were both decreasing in the same order (EC > EDRL > PLGA). SFD-NCM of the lipid nanostructures showed high values of d_{50} (d_{50} values were 15 μm and 62 μm for SLN and LNC, respectively), which are not suitable for pulmonary deposition.

3.5. Bulk density and flowability

Measurement of the bulk density (ρ_{bulk}) of the SD- and SFD-NCM revealed that the SFD-NCM had 10 times lower densities than the corresponding SD-NCM (Table 2). The bulk densities of the SFD-NCM were about 0.02 g/cm³, while the corresponding SD-NCM had bulk densities of about 0.2 g/cm³. Moreover, the values of the CI of SD-NCM showed passable to poor flowability (CI = 22–28), while those of the SFD-NCM showed excellent to good flowability (CI = 6–14). Accordingly, more SFD powder is expected to empty from the capsules and inhaler than the SD powder.

3.6. Specific surface area

Results of the specific surface area measurement using the multipoint BET method are shown in Table 2. As expected, the specific surface areas of the SFD-NCM (60–77 m²/g) were much larger than those of the SD-NCM (1.8–2.4 m²/g).

3.7. Aerodynamic performance

The NGI dispersion data for the SD- and SFD-NCM are plotted in Figs. 4 and 5, respectively. Although the EFs of SFD powders were higher (EF_{SFD} = $97.9 \pm 0.9\%$, while EF_{SD} = $86.4 \pm 2.9\%$), the PPFs of both powders were approximately the same. SD-NCM of polymeric nanoparticles showed PPF values ranging from 35% to 40%, while the corresponding SFD samples showed PPF values ranging from 43% to 46%. Inspection of the NGI data in Figs. 4 and 5 shows that, the SD samples were deposited primarily in the capsules, inhaler and induction port, while SFD samples were deposited primarily in the induction port and the pre-separator. The deposition was very similar in stages 1–5. However, the amounts deposited in the lower stages (stages 6, 7 and MOC) were higher with SFD powders. NGI dispersion data of the SFD-NCM of lipid nanocarriers revealed that most of the powder was deposited in the induction port and the pre-separator, showing lower PPF values (13% and 2% for SLN and LNC, respectively).

Processing the NGI data also allowed the determination of the MMAD values for the powders (Table 2). For SD microcarriers, proximity between d_{50} and MMAD was found, while for SFD microcarriers, a clear difference was found between their large physical diameters ($d_{50} \approx 9\text{--}12$ μm for NCM of polymeric NP), and their smaller aerodynamic diameters (MMAD ≈ 3 μm for NCM of polymeric NP).

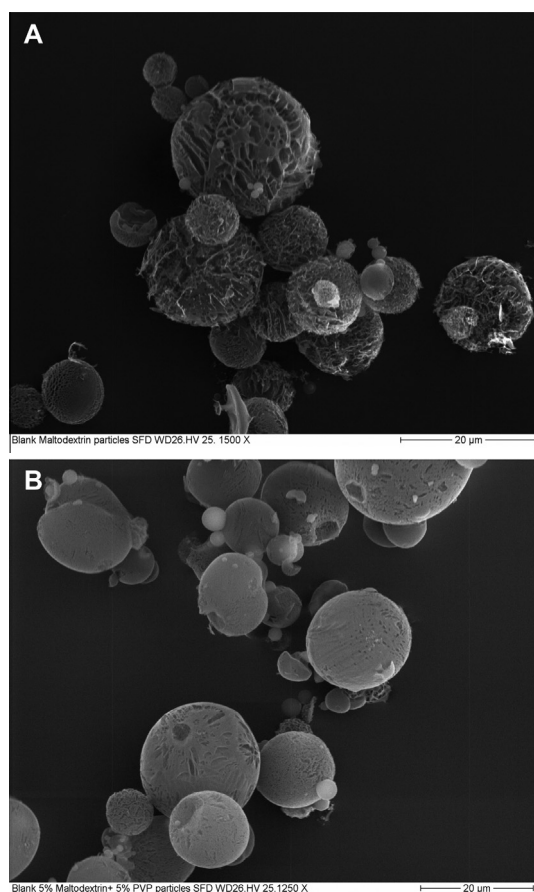


Fig. 1. SEM images of SFD-NCM of: (A) maltodextrin; (B) maltodextrin + PVP.

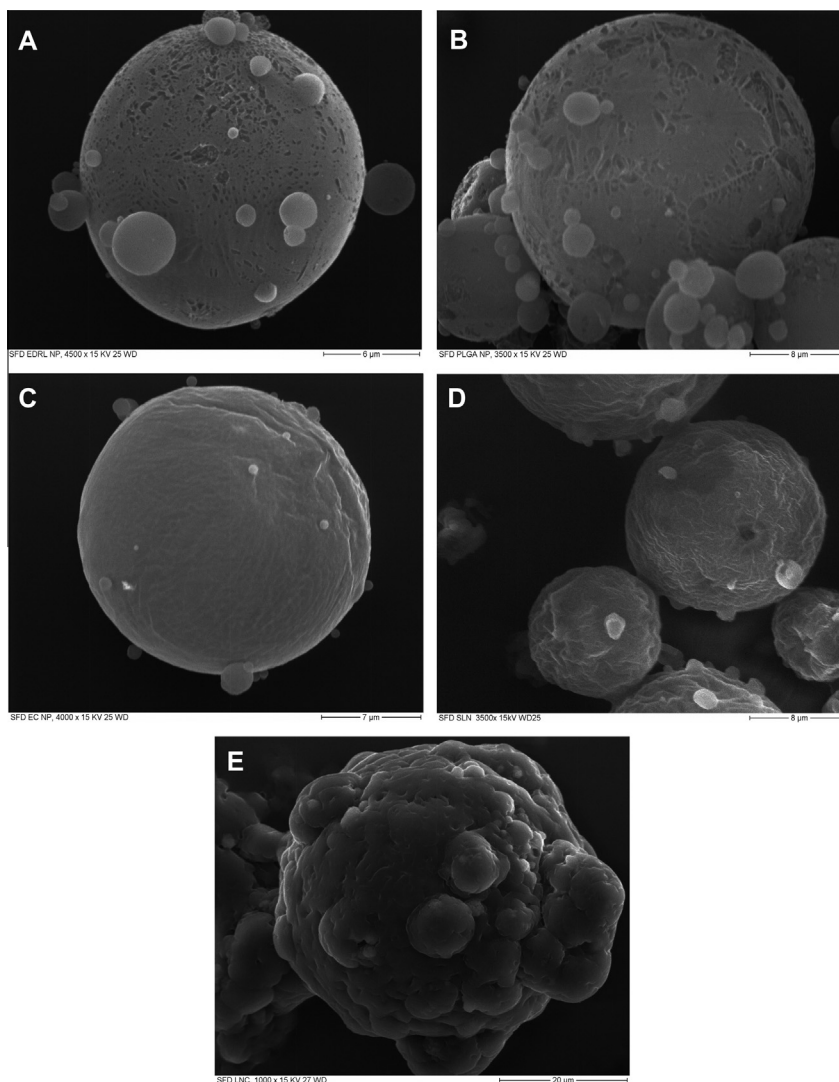


Fig. 2. SEM images of SFD-NCM of: (A) EDRL nanoparticles; (B) PLGA nanoparticles; (C) EC nanoparticles; (D) SLN; (E) LNC.

3.8. Reconstitution of nanoparticles from NCM

Values of the S_f/S_i for the different nanostructures after reconstitution from their corresponding NCM are shown in Fig. 6. All SFD-NCM showed complete reconstitution of the nanoparticles as reflected by the S_f/S_i ratio ($S_f/S_i \approx 1$), except that for LNC which was little higher but still within the range for good reconstitution ($S_f/S_i < 1.5$). On the other hand, SD-NCM only allowed poor reconstitution of nanoparticles as reflected by the high S_f/S_i values ($S_f/S_i = 5.2$ and 2.9 for SD-NCM of PLGA and EC NP, respectively), with the only exception of the SD-NCM of EDRL nanoparticles, which showed complete reconstitution after spray drying ($S_f/S_i \approx 1$).

4. Discussion

Nanoparticle delivery to the lungs has many challenges concerning formulation stability due to particle–particle interactions and the poor deposition efficiency due to exhalation of low-inertia nanoparticles. Thus, incorporating nanoparticles into micron-scale structures is a promising approach to overcome these problems. Such microcarriers should primarily have characteristics suitable for deposition in the deep airways. Secondly, they should

allow the easily reconstitution of the nanostructures with the preservation of their size and colloidal characteristics.

Many techniques have been described for the preparation of NCM suitable for the dry powder inhalation of nanoparticles, including: Spray drying fluidized bed granulation [23], flocculation of oppositely charged nanoparticles [24], dry powder coating [23] and spray drying [7,8,11–13,15]. However, most of these techniques still subject the nanoparticles to harsh conditions such as high temperature, shear stress or milling. For example, the high temperature employed during the commonly used SD caused melting of LNC and SLN because of their lipid core. Moreover, it has been reported that both high temperatures and shear forces increase the kinetic energy of the system during spray drying of SLN, probably based on rapid particle collision, and partially modifying the surfactant film at the interface [6]. Subsequently, NCM preparation of lipid nanocarriers was not possible using SD. For SD at lower inlet and outlet temperatures, an organic solvent or aqueous ethanol solution is frequently used as a SD medium [6,11,13,14]. However, this is not applicable to lipid-soluble components of the nanoparticles. Moreover, insufficiently dry product may be obtained in this case. A valuable alternative could be SFD as proposed here for the production of NCM suitable for pulmonary inhalation. SFD has the advantage that spraying is carried out at low temperature, making it suitable for such formulations with a

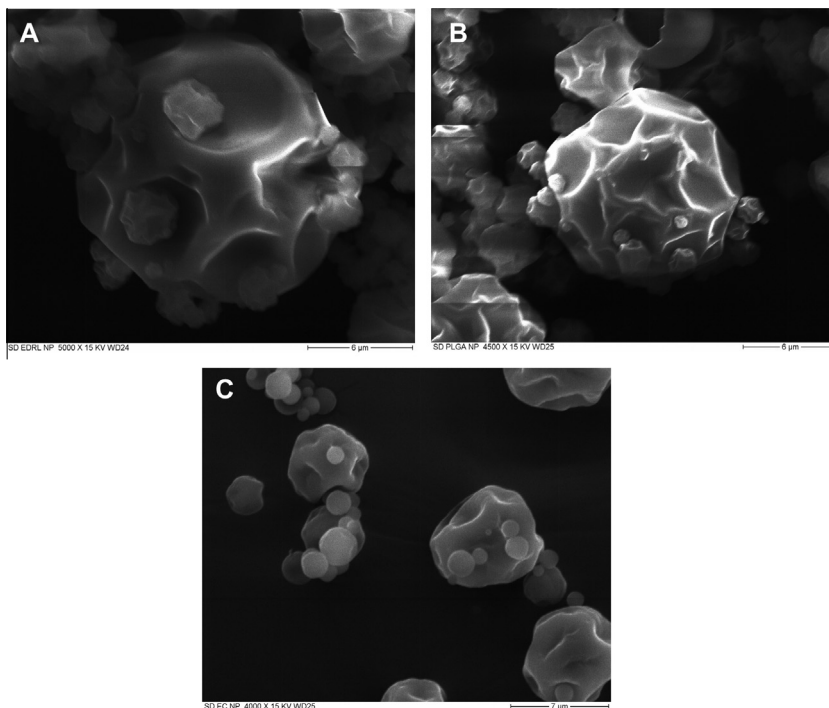


Fig. 3. SEM images of SD-NCM of: (A) EDRL nanoparticles; (B) PLGA nanoparticles; (C) EC nanoparticles.

Table 2
Physical characterization of the prepared SD- and SFD-NCM.

Type of NP/method of preparation	d ₅₀ (μm)	Span	Specific surface area (m ² /g)	ρ _{bulk} (g/cm ³)	CI	MMAD	GSD
EC NP/SD	7.2 ± 0.4	2.2 ± 0.03	2.4 ± 0.2	0.27 ± 0.002	28.3 ± 4.4	3.1 ± 0.1	2.9 ± 0.1
EDRL NP/SD	6.2 ± 0.1	1.6 ± 0.04	2.2 ± 0.1	0.25 ± 0.002	25.5 ± 2.0	3.4 ± 0.5	2.9 ± 0.2
PLGA NP/SD	5.2 ± 0.03	1.9 ± 0.01	1.8 ± 0.1	0.24 ± 0.006	22.1 ± 2.7	3.3 ± 0.1	2.9 ± 0.1
EC NP/SFD	12.3 ± 0.5	2.2 ± 0.1	77.6 ± 0.9	0.02 ± 0.002	7.7 ± 0.6	2.4 ± 0.1	3.1 ± 0.002
EDRL NP/SFD	10.6 ± 0.5	2.6 ± 0.1	67.8 ± 1.9	0.02 ± 0.001	9.6 ± 0.7	3.2 ± 0.2	3.2 ± 0.1
PLGA NP/SFD	9.3 ± 0.4	2.6 ± 0.04	77.1 ± 1.9	0.02 ± 0.001	6.2 ± 1.9	3.4 ± 0.3	3.1 ± 0.1
SLN/SFD	15.4 ± 0.9	1.9 ± 0.02	61.4 ± 1.3	0.07 ± 0.003	7.9 ± 0.7	7.1 ± 2.3	3.6 ± 0.003
LNC/SFD	62.3 ± 5.2	1.9 ± 0.1	60.2 ± 1.2	0.07 ± 0.001	14.7 ± 3.4	14.2 ± 2.6	2.9 ± 0.1

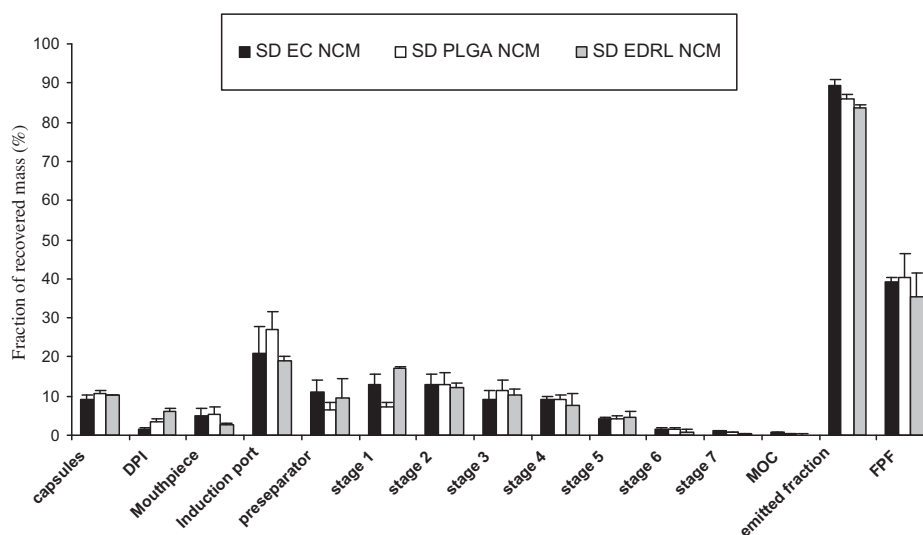


Fig. 4. NGI dispersion data of SD-NCM of polymeric nanoparticles. Data presented as mean ± standard deviation (n = 3).

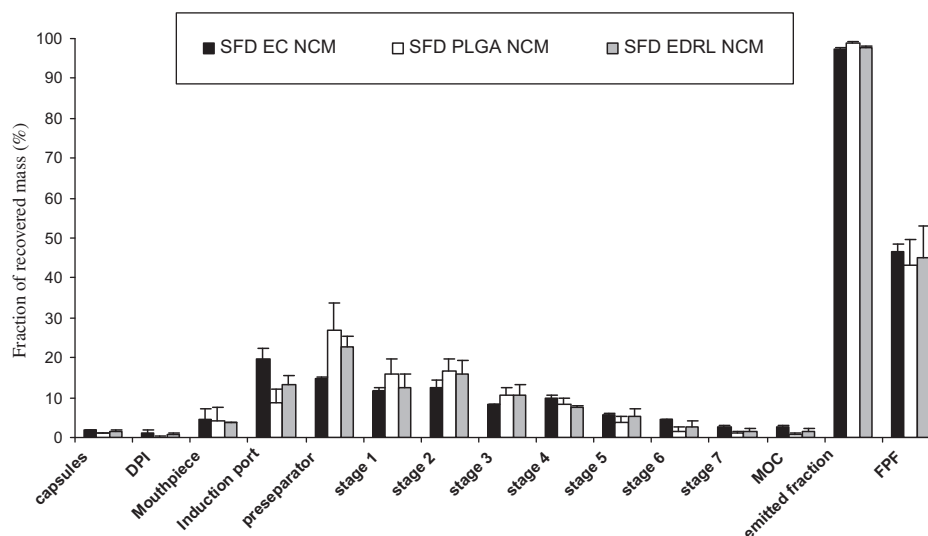


Fig. 5. NGI dispersion data of SFD-NCM of polymeric nanoparticles. Data presented as mean \pm standard deviation ($n = 3$).

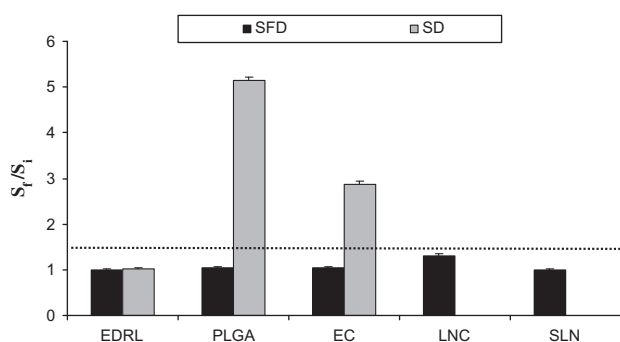


Fig. 6. Effect of SFD and SD on the size of the investigated colloidal nanoparticles.

lipid core, thermally sensitive polymeric nanoparticles, and/or biological macromolecules [14,25].

Another advantage of SFD is the porous structure of the SFD-NCM (as revealed from the SEM images) which facilitates the fast dissolution of the NCM and the release of the nanoparticles in the aqueous environment of the airways. The difference in size, density, specific surface area and morphology between SD- and SFD-NCM can be attributed to the process of particle formation in both cases. During SFD, droplets are frozen, leading to the formation of ice crystals throughout the frozen particle. These ice crystals are then removed during freeze drying leading to interconnected porous particles [26,27]. However, in SD liquid feed is sprayed in a stream of hot gas which evaporates water rapidly causing shrinkage of the droplets and the outer surface solidifies, resulting in particles with smaller size and non-porous surface [26,28].

One of the crucial factors that determine the success of the inhalable dry powder formulations is the aerodynamic performance which strongly affects the lung deposition of the powders. The prepared SFD particles possess low aerodynamic diameters despite their large geometric diameters because of their low densities [27,29–31]. The low density, which owed to either hollow or porous morphologies, causes their aerodynamic diameter to fall within the range suitable for effective lung depositions. Moreover, the prepared SFD-NCM seems to have a higher sphericity and a larger diameter than the corresponding SD-NCM, accordingly a lower aggregation tendency and better flowability (lower CI values) than the SD-NCM is expected. Consequently, more SFD powder emptied

from the capsule and inhaler than the SD powder, as revealed by the higher EF and better deposition in the lower stages of NGI. However, some large particles were likely to exist in the emitted SFD powders which were deposited in the induction port and the preseparator. This was reflected in the similar FPFs of both powders [32].

After deposition, the NCM should have the ability to reconstitute into individual nanoparticles in the aqueous environment of the airways lumen. This is crucial for the nanoparticles to evade the lung clearance mechanisms, therefore maintaining their therapeutic functions. It should be noted that both SD and SFD subject the encapsulated nanoparticles to thermal and/or shear stresses. However, the effect of shear stress was aggravated by the presence of high temperatures in case of SD. The spray dryer is typically operated at inlet temperatures ≥ 100 °C with outlet temperatures in the range of 60–70 °C to achieve a fast convective drying rate. This high temperature can jeopardize the structural integrity of the nanoparticles especially when the glass transition temperature of the polymer is exceeded, even in the presence of drying adjuvant, leading to nanoparticle degradation and melting which diminish their therapeutic functions [7,33]. The poor aqueous re-dispersibility (S_f/S_i ratio >1.5) of some SD-NCM can be attributed to the irreversible nanoparticles aggregation in case of PLGA and EC nanoparticles. In contrast, owing to the low temperatures employed, all SFD-NCM were able to reconstitute the encapsulated nanoparticles (S_f/S_i ratio <1.5). This can be explained on the basis that the particles were able to withstand the shear stress during SFD and the presence of cryoprotectant preserved the particles from the various stresses during freezing and dehydration steps. The immobilization of nanoparticles within a glassy matrix of cryoprotectant can prevent their aggregation and protect them against the mechanical stress of ice crystals [34]. Moreover, the presence of a crystallization inhibitor such as PVP in the formulation helped to maintain the amorphous state of both nanoparticles and the cryoprotectant.

For SFD of formulations containing high surfactant concentrations (such as LNC and SLN), the shape, size and accordingly the aerodynamic properties of the particles are dependent on the amount of free surfactants remaining in the formulation. Liquid break up causes an increase in the gas/liquid interface and the free surface energy. However, the high surfactant concentrations in the formulation, as in case of LNC, would lower the surface tension between the droplets and the surrounding air. In this case, multiple

droplets tend to coalesce together, giving particles which are larger in size and/or irregular in shape, depending on the amount of free surfactants.

5. Conclusions

SFD is a promising approach for the preparation of inhalable NCM. With regard to the feasibility of formulation, both polymeric and lipid nanocarriers were successfully formulated as NCM using the SFD technique. Moreover, SFD produces low-density porous NCM, possessing low aerodynamic diameters and suitable for pulmonary deposition. In contrast to SD, SFD is the method of choice when the reconstitution of the encapsulated nanocarriers is the main concern.

Acknowledgments

Mohamed Ehab Ali would like to acknowledge the Egyptian Ministry of Higher Education and the German Academic Exchange Service (Deutsche Akademische Austauschdienst, DAAD) for the financial support (A/09/92434). Alf Lamprecht is thankful to the 'Institut Universitaire de France'. The authors are also very grateful for the financial support of the "Deutsche Forschungsgemeinschaft" (DFG) in the framework of SPP1423 (Grant no. LA1362/2).

References

- [1] H.M. Courrier, N. Butz, T.F. Vandamme, Pulmonary drug delivery systems: recent developments and prospects, *Crit. Rev. Ther. Drug Carrier Syst.* 19 (2002) 425–498.
- [2] S. Gill, R. Lobenberg, T. Ku, S. Azarmi, W. Roa, E.J. Prenner, Nanoparticles: characteristics, mechanisms of action, and toxicity in pulmonary drug delivery – a review, *J. Biomed. Nanotechnol.* 3 (2007) 107–119.
- [3] P.G. Roveda, D. Traini, The nanoscale in pulmonary delivery. Part 1: deposition, fate, toxicology and effects, *Expert Opin. Drug Deliv.* 4 (2007) 595–606.
- [4] W. Yang, J.I. Peters, R.O. Williams 3rd, Inhaled nanoparticles – a current review, *Int. J. Pharm.* 356 (2008) 239–247.
- [5] L.A. Dailey, T. Schmehl, T. Gessler, M. Wittmar, F. Grimminger, W. Seeger, T. Kissel, Nebulization of biodegradable nanoparticles: impact of nebulizer technology and nanoparticle characteristics on aerosol features, *J. Contr. Release* 86 (2003) 131–144.
- [6] C. Freitas, R.H. Mullera, Spray-drying of solid lipid nanoparticles (SLN TM), *Eur. J. Pharm. Biopharm.* 46 (1998) 145–151.
- [7] T. Lebbhardt, S. Roesler, H.P. Uusitalo, T. Kissel, Surfactant-free redispersible nanoparticles in fast-dissolving composite microcarriers for dry-powder inhalation, *Eur. J. Pharm. Biopharm.* 78 (2011) 90–96.
- [8] S. Al-Qadi, A. Grenha, D. Carrion-Recio, B. Seijo, C. Remunan-Lopez, Microencapsulated chitosan nanoparticles for pulmonary protein delivery: in vivo evaluation of insulin-loaded formulations, *J. Contr. Release* 157 (2012) 383–390.
- [9] A. Grenha, B. Seijo, C. Remunan-Lopez, Microencapsulated chitosan nanoparticles for lung protein delivery, *Eur. J. Pharm. Sci.* 25 (2005) 427–437.
- [10] J.O. Sham, Y. Zhang, W.H. Finlay, W.H. Roa, R. Lobenberg, Formulation and characterization of spray-dried powders containing nanoparticles for aerosol delivery to the lung, *Int. J. Pharm.* 269 (2004) 457–467.
- [11] F. Ungaro, I. d'Angelo, C. Coletta, R. d'Emmanuele di Villa Bianca, R. Sorrentino, B. Perfetto, M.A. Tufano, A. Miro, M.I. La Rotonda, F. Quaglia, Dry powders based on PLGA nanoparticles for pulmonary delivery of antibiotics: modulation of encapsulation efficiency, release rate and lung deposition pattern by hydrophilic polymers, *J. Contr. Release* 157 (2012) 149–159.
- [12] D.K. Jensen, L.B. Jensen, S. Koocheki, L. Bengtson, D. Cun, H.M. Nielsen, C. Foged, Design of an inhalable dry powder formulation of DOTAP-modified PLGA nanoparticles loaded with siRNA, *J. Contr. Release* 157 (2012) 141–148.
- [13] M. Beck-Broichsitter, C. Schweiger, T. Schmehl, T. Gessler, W. Seeger, T. Kissel, Characterization of novel spray-dried polymeric particles for controlled pulmonary drug delivery, *J. Contr. Release* 158 (2012) 329–335.
- [14] Y. Wang, K. Kho, W.S. Cheow, K. Hadinoto, A comparison between spray drying and spray freeze drying for dry powder inhaler formulation of drug-loaded lipid-polymer hybrid nanoparticles, *Int. J. Pharm.* 424 (2012) 98–106.
- [15] N. Tsapis, D. Bennett, B. Jackson, D.A. Weitz, D.A. Edwards, Trojan particles: large porous carriers of nanoparticles for drug delivery, *Proc. Natl. Acad. Sci. USA* 99 (2002) 12001–12005.
- [16] S.N. Eggerstedt, M. Dietzel, M. Sommerfeld, R. Suverkrup, A. Lamprecht, Protein spheres prepared by drop jet freeze drying, *Int. J. Pharm.* 438 (2012) 160–166.
- [17] M.M. Abdel-Mottaleb, D. Neumann, A. Lamprecht, Lipid nanocapsules for dermal application: a comparative study of lipid-based versus polymer-based nanocarriers, *Eur. J. Pharm. Biopharm.* 79 (2011) 36–42.
- [18] V. Hoffart, N. Ubrich, C. Simonin, V. Babak, C. Vigneron, M. Hoffman, T. Lecompte, P. Maincent, Low molecular weight heparin-loaded polymeric nanoparticles: formulation, characterization, and release characteristics, *Drug Develop. Ind. Pharm.* 28 (2002) 1091–1099.
- [19] A. Lamprecht, J.L. Saumet, J. Roux, J.P. Benoit, Lipid nanocarriers as drug delivery system for ibuprofen in pain treatment, *Int. J. Pharm.* 278 (2004) 407–414.
- [20] B. Heurtault, P. Saulnier, B. Pech, J.E. Proust, J.P. Benoit, A novel phase inversion-based process for the preparation of lipid nanocarriers, *Pharm. Res.* 19 (2002) 875–880.
- [21] M.A. Casadei, F. Cerreto, S. Cesa, M. Giannuzzo, M. Feeney, C. Marianecchi, P. Paolicelli, Solid lipid nanoparticles incorporated in dextran hydrogels: a new drug delivery system for oral formulations, *Int. J. Pharm.* 325 (2006) 140–146.
- [22] K. Kho, K. Hadinoto, Aqueous re-dispersibility characterization of spray-dried hollow spherical silica nano-aggregates, *Powder Technol.* 198 (2010) 354–363.
- [23] M. Yang, H. Yamamoto, H. Kurashima, H. Takeuchi, T. Yokoyama, H. Tsujimoto, Y. Kawashima, Design and evaluation of poly(DL-lactic-co-glycolic acid) nanocomposite particles containing salmon calcitonin for inhalation, *Eur. J. Pharm. Sci.* 46 (2012) 374–380.
- [24] L. Shi, C.J. Plumley, C. Berkland, Biodegradable nanoparticle flocculates for dry powder aerosol formulation, *Langmuir* 23 (2007) 10897–10901.
- [25] Z.L. Wang, W.H. Finlay, M.S. Peppler, L.G. Sweeney, Powder formation by atmospheric spray-freeze-drying, *Powder Technol.* 170 (2006) 45–52.
- [26] J.P. Amorij, J. Meulenaar, W.L. Hinrichs, T. Stegmann, A. Huckriede, F. Coenen, H.W. Frijlink, Rational design of an influenza subunit vaccine powder with sugar glass technology: preventing conformational changes of haemagglutinin during freezing and freeze-drying, *Vaccine* 25 (2007) 6447–6457.
- [27] Y.F. Maa, P.A. Nguyen, T. Sweeney, S.J. Shire, C.C. Hsu, Protein inhalation powders: spray drying vs spray freeze drying, *Pharm. Res.* 16 (1999) 249–254.
- [28] Y.F. Maa, H.R. Costantino, P.A. Nguyen, C.C. Hsu, The effect of operating and formulation variables on the morphology of spray-dried protein particles, *Pharm. Develop. Technol.* 2 (1997) 213–223.
- [29] S.M. D'Addio, J.G. Chan, P.C. Kwok, R.K. Prud'homme, H.K. Chan, Constant size, variable density aerosol particles by ultrasonic spray freeze drying, *Int. J. Pharm.* 427 (2012) 185–191.
- [30] M. Wahjudi, S. Murugappan, R. van Merkerk, A.C. Eissens, M.R. Visser, W.L.J. Hinrichs, W.J. Quax, Development of a dry, stable and inhalable acyl-homoserine-lactone-acylase powder formulation for the treatment of pulmonary *Pseudomonas aeruginosa* infections, *Eur. J. Pharm. Sci.* 48 (2013) 637–643.
- [31] G. Sharma, W. Mueannoom, A.B. Buanz, K.M. Taylor, S. Gaisford, In vitro characterisation of terbutaline sulphate particles prepared by thermal ink-jet spray freeze drying, *Int. J. Pharm.* 447 (2013) 165–170.
- [32] W. Liang, P.C. Kwok, M.Y. Chow, P. Tang, A.J. Mason, H.K. Chan, J.K. Lam, Formulation of pH responsive peptides as inhalable dry powders for pulmonary delivery of nucleic acids, *Eur. J. Pharm. Biopharm.* (2013).
- [33] W.S. Cheow, M.L. Ng, K. Kho, K. Hadinoto, Spray-freeze-drying production of thermally sensitive polymeric nanoparticle aggregates for inhaled drug delivery: effect of freeze-drying adjuvants, *Int. J. Pharm.* 404 (2011) 289–300.
- [34] W. Abdelwahed, G. Degobert, S. Stainmesse, H. Fessi, Freeze-drying of nanoparticles: formulation, process and storage considerations, *Adv. Drug Deliv. Rev.* 58 (2006) 1688–1713.